IEEE Access
Multidisciplinary | Rapid Review | Open Access Journal

Received 10 May 2023, accepted 21 May 2023, date of publication 29 May 2023, date of current version 15 June 2023.

Digital Object Identifier 10.1109/ACCESS.2023.3280979

RESEARCH ARTICLE

A Novel Iterative Second-Order Neural-Network Learning Control Approach for Robotic Manipulators

DANG XUAN BA[1], (Member, IEEE), NGUYEN TRUNG THIEN[2], AND JOONBUM BAE[3], (Member, IEEE)

[1]Department of Automatic Control, HCMC University of Technology and Education, Ho Chi Minh City 71300, Vietnam
[2]Viettel Manufacturing Corporation, Hanoi 11106, Vietnam
[3]Department of Mechanical Engineering, Ulsan National Institute of Science and Technology, Ulsan 44919, South Korea

Corresponding author: Joonbum Bae (jbbae@unist.ac.kr)

This work was supported by the Ministry of Education and Training, Ho Chi Minh City University of Technology and Education, Vietnam, under Project B2021-SPK-03.

ABSTRACT Iterative Learning Control (ILC) is known as a high-accuracy control strategy for repetitive control missions of mechatronic systems. However, applying such learning controllers for robotic manipulators to result in excellent control performances is now a challenge due to unstable behaviors coming from nonlinearities, uncertainties and disturbances in the system dynamics. To tackle this challenge, in this paper, we present a novel proportional-derivative iterative second-order neural-network learning control (PDISN) method for motion-tracking control problems of robotic manipulators. The control framework is structured from time- and iterative-base control layers. First of all, the total systematic dynamics are concretely stabilized by a conventional Proportional-Derivative (PD) control signal in the time domain. The control objective is then accomplished by using an intelligent ILC decision generated in the second layer to compensate for other nonlinear uncertainties and external disturbances in the dynamics. The iterative signal is flexibly composed from various information on the iterative axis. On one hand, the previous iterative control signal is inherently reused in the current iteration but with an appropriate portion based on reliability of the current control performance. On the other hand, the iterative-based modeling deviation remaining is treated by a functional neural network that is specially activated by a second-order learning law and information synthesized from the current and previous iterations. Stabilities of the time-based nonlinear subsystem and overall system are rigorously analyzed using extended Lyapunov theories and high-order regression series criteria. Effectiveness of the proposed controller was intensively verified by the extensive comparative simulation results. Key advantages of the proposed control method are chattering-free, universal, adaptive, and robust.

INDEX TERMS Iterative learning control, motion control, neural networks, robotic manipulators.

I. INTRODUCTION

Recently, robots play an indispensable role in industry and day-life activities [1], [2], [3]. Furthermore, they can cowork with humans to increase working efficiency [2], [4]. As a result, such modern robots have to possess high control accuracies, adaptation, robustness and reliability [1], [3]. However, unknown dynamical influences and complicated working environments are barriers degrading outstanding control performances [8], [9], [10], [11]. Proportional-Integral-Derivative (PID) controllers have been mostly equipped in industrial robots thanks to their simplicity in implementation, strong robustness and acceptable control performances [1], [5], [6], [7]. To deal with nonlinearities and uncertainties in the system dynamics for higher control precision, model-based controllers have been studied

The associate editor coordinating the review of this manuscript and approving it for publication was Wei Liu.

using typical physical analyses such as Newton, Euler or Lagrange methods, or decomposition principles [12], [13]. In practice, applicability of such conventional approaches is limited for general robots. By utilizing universal approximation properties, neural-network-based control methods are growingly employed in servo systems [14], [15], [16]. Direct and indirect adaptation laws have been successfully adopted to activate neural networks in automatic control systems [10], [17]. The systematic behaviors could be well captured by neural networks, and their results could be then employed to compensate for unknown dynamics in control processes. Such design could be applied to divergent types of neural network such as Radial-basis function (RBF) networks [14], [18], [19] or Fuzzy-hybrid-networks [20], [21]. Remarkable control outcomes have been delivered by the intelligent controllers. For repetitive tasks that frequently occur in industrial activities, time-based neural-network-based control approaches could be modified to result in higher control accuracies [22], [23]. This demand was the key motivation of ILC approaches [24], [25].

Nowadays, ILC becomes a famous control framework for systems required repetitive missions. Its basic idea is that an iterative control signal is computed based on errors from previous trails to optimize working performance of control systems. With simple design, it could demonstrate superior performances thanks to an unique nature in effectively dealing with repetitive disturbances such as gravity and model uncertainties [26], [27]. In [29], a simple ILC controller was successfully applied for a cable-driven robot. However, it required another homing controller to steer the initial control errors back to zero before the ILC control signal went to operation, and the stability of the closed-loop system was difficult to be maintained in high-speed control regions. In fact, disturbances and dynamical uncertainties in the system models are rarely repetitive terms. In most robotic systems, both iteration-variant and iteration-invariant disturbances exist on the iterative direction. External torques and internal state-dependent disturbances can be grouped into iterative-variant disturbances while uncertain parameters such as link masses or external loads can be considered as iteration-invariant disturbances. To extensively deal with the iterative disturbances, a lot of interesting ILC approaches have been developed. ILC methods with robust learning filters, such as frequency or time-frequency filters, were employed to isolate nonrepetitive disturbances from the iterative loop. In [23], low-pass filters were employed to treat model uncertainties at high frequencies. In [34], a notch Q filter and a disturbance observer were combined in the ILC to detach external vibration disturbances at certain frequencies. In [35], a time-frequency numerical Q filter was proposed to eliminate the iteration-variant disturbances. In [36], a new robust Q-filter-based ILC approach was adopted incorporated with a feedback control signal to deal with both repetitive and nonrepetitive perturbances.

Due to complicated working behaviors and multiple dimensional characteristics, advanced ILC methods are required for robotic applications. To effectively eliminate iterative disturbances in general robotic dynamics, an adaptive iterative learning control (AILC) method was proposed in [22] based on Lyapunov analyses. As reported in [37] and [38], the AILC framework adopted an adaptive signal which iteratively approximated and attenuated unknown disturbances and uncertainties in the system dynamics. However, the algorithm was restricted on a need that the parameters were assumed to be constants within each iteration [39], [40]. To increase flexibility of the AILC structure for robotic systems, in [30] and [62], new ILC approaches were studied in which data-driven learning laws were adopted to compensate for the systematic uncertainties and to accelerate convergence rates. Unfortunately, since the data-driven ILC methods were designed based on linear time-variant models, they were only applied either to generate referenced joint velocities of general robotic control systems or to control simple mechatronic systems such as gantry robots that have joints in orthogonal configurations and independent control structures. In [31] and [32], other AILC remedies were employed for robotic manipulators in which the optimal iterative control gains of the conventional ILC were found by solving optimization problems. However, the control plants were required to be formatted in a linear time-variant forms and initial conditions of the control errors had to set to be the same values. They thus limit strong power of the new AILC for robotic systems. Besides, ILC schemes were incorporated with a time-based adaptive control rule to provide promising control results [31], [41], [61]. Evaluation results reveal that the good control results were obtained mainly from the achievement of the time-based control signals in low frequencies and from the iterative-based structure in high frequencies. However, stabilities of the closed-loop systems under operation of the time-based control signals need to be further investigated [31], [61]. Several different research directions of the ILC design have been attempted in which the learning information were collected in the current iteration [38], [42], [43]. Excellent control results were published, but using model-based learning laws hindered their wide-spread applicability [41], [44]. As a trend, ILC research based on operation of neural networks for robotic systems has been noticed in recent times. In [45], systematic disturbances in the current iteration were estimated by a pulse-based neural network and they were then fed to the control phase for improving the control performance on the iteration axis. Initial resetting problems and reliability of the neural ILC approach was then treated by a new saturation neural network built up from the present iteration [16]. From the above analyses, it can be seen that iterative disturbances are state-, time- and iterative-dependent factors [23], [41]. In [33], lumped iterative disturbances were eliminated by PD discontinuous iterative rules. Potential of the nonlinear ILC approach was confirmed by verification results obtained, but its benefits

were only valid in the same initial conditions of the iterative control errors and in a class of iterative disturbances that were proportional to joint velocities. Designing a simple iterative control signal that can well suppress all of nonlinearities, uncertainties and disturbances in the systematic dynamics for outstanding control performances is really a very interesting challenge.

To fill out this gap with a simple-yet-universal method, in this paper, we propose a rigorous universal ILC approach for robotic manipulators using a functional neural network. The controller is structured by two control layers: a time-based control layer and an iterative-based control layer. Innovative design of the proposed control method is presented with the following contributions:

- A stabilization control signal for the manipulator is designed based on a simple PD control error associated with a concrete support Lyapunov theory.
- The control performance is then further enhanced by a novel ILC framework in which the iterative control signal is flexibly updated based on reliability of the current control performance, and iterative disturbances are eliminated by a neural network with an appropriate learning procedure. The neural network is operated based on both previous and current iterative information under a special second-order adaptation rule.
- Stability and effectiveness of the closed-loop system are carefully verified by Lyapunov constraints, regression series criteria and intensive simulation discussions.

The proposed controller holds important characteristics: initial-resetting treatment, model-free design, smooth control signals, adaptation, robustness and high accuracies. Outline of the paper is organized as follows. System dynamics are briefly reviewed, and problem statements are then defined in *Section II*. Detailed design of the controller and stability analyses of the overall system are presented in *Section III*. Effectiveness of the proposed control system is discussed in *Section IV*. Conclusions are finally noted in *Section V*.

Throughout this paper, for simplicity, we adopt the following abbreviation: **bold U**pper-case, **bold l**ower-case, *italic l*ower-case characters respectively denote **Matrix**, **vector** and *scalar* functions or variables; If a function is presented in both lower-case and upper-case formations, the lower-case one denotes elements of the upper-case one; The term $(x = x\lfloor\bullet\rfloor)$ denote a function of $(\bullet)$; $(\lambda_\bullet = eig\lfloor\bullet\rfloor)$ is an eigen value of matrix $(\bullet)$; $(\bar{\bullet} = max\lfloor\bullet\rfloor)$ and $(\underline{\bullet} = min\lfloor\bullet\rfloor)$ are maximum and minimum values of $(\bullet)$, respectively.

II. SYSTEM MODELING AND PROBLEM STATEMENTS

Dynamics of a general n-Degree-Of-Freedom (n-DOF) robot are expressed using the following equation [9], [12], [13]:

$$M\lfloor q\rfloor\ddot{q} = -C\lfloor q,\dot{q}\rfloor\dot{q} - g\lfloor q\rfloor + f\lfloor\dot{q}\rfloor + \tau_d + \tau \quad (1)$$

where $q,\ \dot{q},\ \tau \in \Re^n$ are vectors of the joint position, angular velocity, and the control torque, respectively, $M \in \Re^{n\times n}$ is the inertia-mass matrix, $C\dot{q},\ g, f, \tau_d \in \Re^n$ stand for the Coriolis/Centripetal effect, the gravitational torque, frictional torque, and external disturbances, respectively.

Remark 1: The dynamical robotic model (1) possesses the following constraints [13], [46]:

Property 1: The term $M\lfloor q\rfloor$ is a symmetric bounded positive-definite matrix.

Property 2: The matrix $C\lfloor q,\ \dot{q}\rfloor$ is linear bounded with respect to the second argument $x_1 \in \Re^n$, a given term $x_2 \in \Re^n$, and a positive constant Δ_0 as follows:

$$\begin{cases} C\lfloor q,x_1\rfloor x_2 = C\lfloor q,x_2\rfloor x_1 \\ C\lfloor q,x_1 + x_2\rfloor = C\lfloor q,x_1\rfloor + C\lfloor q,x_2\rfloor \\ C\lfloor q,x_1\rfloor x_2 \le \Delta_0\|x_1\|\,\|x_2\| \end{cases} \quad (2)$$

Property 3: The gravitational vector $g\lfloor q\rfloor$ is bounded.

Property 4: The Coriolis/centripetal matrix $C\lfloor q,\ \dot{q}\rfloor$ and the time derivative of the mass matrix $M\lfloor q\rfloor$ satisfy the skew-matrix constraint:

$$y^T\left(\dot{M}\lfloor q\rfloor - 2C\lfloor q,\dot{q}\rfloor\right)y = 0 \qquad \forall y, q, \dot{q} \in \Re^n \quad (3)$$

Property 5: The frictional term $f\lfloor\dot{q}\rfloor$ can be linearized as

$$f(\dot{q}) = -\Gamma\dot{q} \quad (4)$$

where Γ is a bounded positive-definite matrix.

Assumption 1: The external disturbance (τ_d) is bounded [23], [47], [48].

Assumption 2: The reference profile (q_d) is a known, repetitive, bounded and twice continuously differentiable signal.

Assumption 3: The system states $(q,\ \dot{q})$ are measurable.

Remark 2: Note that the external disturbance (τ_d) denotes unmodeled terms and projection of external forces/torques acting to the robot body at any points on the system dynamics [13]. We define a tracking control error composited from the desired signal (q_d) and the system output (q). The control mission here is to develop an intelligent nonlinear controller to accomplish excellent tracking control precision. Challenges of this work come from unknown unstable internal dynamical behaviors and complex external disturbances affecting to the system during the operation process. However, one advantage of the control system is that it can run in many iterations. Other advanced features of the controller are adaptation and robustness.

III. PROPORTIONAL-DERIVATIVE ITERATIVE SECOND-ORDER NEURAL-NETWORK LEARNING CONTROLLER (PDISN)

In this section, the designing process of the proposed control idea is presented with a simple PD control procedure and an advanced ILC approach. Respective theoretical proof is also provided to clarify effectiveness of the developed features.

The main control objective is mathematically synthesized as follows:

$$e = q - q_d \quad (5)$$

To realize the tracking control requirement, the final control signal is simply selected as [38], [41]:

$$\tau = \tau_t + \tau_i \tag{6}$$

where τ_t and τ_i are time-based and iterative-base control terms, respectively.

A. TIME-BASED PD CONTROL SIGNAL

In literature, various types of linear or nonlinear control design were employed for high-precision control of the manipulators [1], [17], [49]. Purpose of the time-based control signal is to stabilize internal/external dynamics of the system (1) and force the control error (5) to be as small as possible. In this mind, the time-domain control signal is designed with a simplest control form using the following PD structure:

$$\tau_t = -K_{Pt} e - K_{Dt} \dot{e} \tag{7}$$

where K_{Pt} and K_{Dt} are diagonal positive-definite gain matrices.

The control signal (7) has been widely used in industrial and researching robots [5], [19], [50]. Stability of the closed-loop PD robotic system is confirmed from previous work [1] based on a linearizing model with many assumptions that might be weak in some cases. In the following statement, complete novel proof is discussed based on a nonlinear Lyapunov approach.

Lemma 1: For any bounded functions $|u| \leq \bar{u}$, $|v| \leq \bar{v}$, there always exist three positive constants $(0 < \rho_u)$, $(0 < \rho_v)$ and $(a > 1)$ complying with the following inequality:

$$2\sqrt{\rho_u \rho_v} \geq u\rho_u^a + v\rho_v \tag{8}$$

Proof:

The inequality (8) is satisfied if the following conditions hold:

$$\begin{cases} \sqrt{\rho_u \rho_v} \geq \bar{u}\rho_u^a \\ \sqrt{\rho_u \rho_v} \geq \bar{v}\rho_v \end{cases} \tag{9}$$

It can be easily seen that the *proof* of *Lemma 1* is completed by selecting the constants satisfying:

$$\begin{cases} 0 < \rho_v \leq \bar{u}^{(-1/(a-1))} \bar{v}^{(-(2a-1)/(a-1))} \\ 0 < \rho_u \leq (\bar{u}\,\bar{v})^{-1/(a-1)} \\ 0 < \bar{v}^2 \rho_v \leq \rho_u \end{cases} \tag{10}$$

□

Theorem 1: By applying the control signals (6)-(7) to the robotic system (1) that possesses *Properties* (1)-(5) under *Assumption* 1, the system output is bounded if the iterative control signal τ_i is bounded.

Proof:

By noting *Property* 5 and the control laws (6)-(7), the closed-loop system is expressed as follows:

$$\begin{aligned} M\ddot{q} = &-C\dot{q} - g - \Gamma\dot{q} + \tau_d - K_{Dt}\,(\dot{q} - \dot{q}_d) \\ &- K_{Pt}\,(q - q_d) + \tau_i \end{aligned} \tag{11}$$

The following Lyapunov function is investigated

$$\begin{aligned} L = &\, 0.5(\dot{q} + \alpha_{t1} q)^T M\,(\dot{q} + \alpha_{t1} q) \\ &+ 0.25\alpha_{t2}\left(\dot{q}^T M \dot{q} + q^T K_{Pt} q + 2\alpha_{t3}\right) \\ &\times \left(\dot{q}^T M \dot{q} + q^T K_{Pt} q\right) \end{aligned} \tag{12}$$

where $\alpha_{tj|j=1,2,3}$ are positive constants.

By invoking the dynamics (11), the time derivative of the candidate function (12) is derived as in (13).

$$\begin{aligned} \dot{L} = &\, 0.5(\dot{q} + \alpha_{t1} q)^T \dot{M}\,(\dot{q} + \alpha_{t1} q) \\ &+ (\dot{q} + \alpha_{t1} q)^T M\,(\ddot{q} + \alpha_{t1}\dot{q}) \\ &+ \alpha_{t2}\left(\dot{q}^T M \dot{q} + q^T K_{Pt} q + \alpha_{t3}\right) \\ &\times \left(0.5\dot{q}^T \dot{M}\dot{q} + \dot{q}^T M \ddot{q} + q^T K_{Pt}\dot{q}\right) \\ = &\, 0.5(\dot{q} + \alpha_{t1} q)^T \dot{M}\,(\dot{q} + \alpha_{t1} q) \\ &+ (\dot{q} + \alpha_{t1} q)^T\,(-C\dot{q} - g - \Gamma\dot{q} + \tau_d) + (\dot{q} + \alpha_{t1} q)^T \\ &\times (-K_{Dt}\,(\dot{q} - \dot{q}_d) - K_{Pt}\,(q - q_d) + \tau_i + \alpha_{t1} M\dot{q}) \\ &+ \alpha_{t2}\left(\dot{q}^T M \dot{q} + q^T K_{Pt} q + \alpha_{t3}\right) \\ &\times \left(0.5\dot{q}^T \dot{M}\dot{q} + q^T K_{Pt}\dot{q} - \dot{q}^T\,(C\dot{q} + g + \Gamma\dot{q})\right) \\ &+ \alpha_{t2}\left(\dot{q}^T M \dot{q} + q^T K_{Pt} q + \alpha_{t3}\right) \\ &\times \left(\dot{q}^T\,(\tau_d - K_{Dt}\,(\dot{q} - \dot{q}_d) - K_{Pt}\,(q - q_d) + \tau_i)\right) \end{aligned} \tag{13}$$

Simplifying the dynamics (13) by using *Properties 1-4* results in (14).

$$\begin{aligned} \dot{L} = &\, (\dot{q} + \alpha_{t1} q)^T\,(\alpha_{t1} C q - g - \Gamma\dot{q} + \tau_d - K_{Dt}\,(\dot{q} - \dot{q}_d)) \\ &+ (\dot{q} + \alpha_{t1} q)^T\,(-K_{Pt}\,(q - q_d) + \tau_i + \alpha_{t1} M\dot{q}) \\ &+ \alpha_{t2}\left(\dot{q}^T M \dot{q} + q^T K_{Pt} q + \alpha_{t3}\right)\left(\dot{q}^T\,(-g - \Gamma\dot{q} + \tau_d)\right) \\ &+ \alpha_{t2}\left(\dot{q}^T M \dot{q} + q^T K_{Pt} q + \alpha_{t3}\right) \\ &\times \left(\dot{q}^T\,(-K_{Dt}\,(\dot{q} - \dot{q}_d) + K_{Pt} q_d + \tau_i)\right) \\ \leq &\, \Delta_0 \alpha_{t1} \|\dot{q}\|^2 \|q\| + \dot{q}^T\,(-g + \tau_d + K_{Dt}\dot{q}_d + K_{Pt} q_d + \tau_i) \\ &- \dot{q}^T K_{Pt} q - \dot{q}^T\,(\Gamma + K_{Dt} - M\alpha_{t1})\,\dot{q} + \Delta_0 \alpha_{t1}^2 \|q\|^2 \|\dot{q}\| \\ &+ \alpha_{t1} q^T\,(-g + \tau_d + K_{Dt}\dot{q}_d + K_{Pt} q_d + \tau_i) \\ &- \alpha_{t1} q^T\,(\Gamma + K_{Dt} - M\alpha_{t1})\,\dot{q} - \alpha_{t1} q^T K_{Pt} q \\ &+ \alpha_{t2}\left(\dot{q}^T M \dot{q} + q^T K_{Pt} q + \alpha_{t3}\right)\left(-\dot{q}^T\,(\Gamma + K_{Dt})\,\dot{q}\right) \\ &+ \alpha_{t2}\left(\dot{q}^T M \dot{q} + q^T K_{Pt} q + \alpha_{t3}\right) \\ &\times \left(\dot{q}^T\,(-g + \tau_d + K_{Dt}\dot{q}_d + K_{Pt} q_d + \tau_i)\right) \\ \leq &\, \Delta_0 \alpha_{t1} \|\dot{q}\|^2 \|q\| + \left(\Delta_0 \alpha_{t1}^2 + \alpha_{t2}\Delta_d \bar{\lambda}_{K_{Pt}}\right) \|q\|^2 \|\dot{q}\| \\ &- \left(\underline{\lambda}_{(\Gamma + K_{Dt} - M\alpha_{t1})} + \alpha_{t2}\alpha_{t3}\underline{\lambda}_{(\Gamma + K_{Dt})}\right) \|\dot{q}\|^2 \\ &+ \alpha_{t2}\Delta_d \bar{\lambda}_M \|\dot{q}\|^3 - \alpha_{t1}\underline{\lambda}_{K_{Pt}} \|q\|^2 \\ &- \alpha_{t2}\underline{\lambda}_M \underline{\lambda}_{(\Gamma + K_{Dt})} \|\dot{q}\|^4 - \alpha_{t2}\underline{\lambda}_{K_{Pt}} \underline{\lambda}_{(\Gamma + K_{Dt})} \|q\|^2 \|\dot{q}\|^2 \\ &+ \bar{\lambda}_{K_{Pt} + \alpha_{t1} K_{Dt} + \alpha_{t1}\Gamma - M\alpha_{t1}^2} \|\dot{q}\| \|q\| \\ &+ \|\dot{q}\|\,\Delta_d\,(1 + \alpha_{t2}\alpha_{t3}) + \alpha_{t1} \|q\|\,\Delta_d \end{aligned} \tag{14}$$

where Δ_d is an upper bound of the systematic perturbance:

$$\Delta_d = \max \lfloor \| -g + \tau_d + K_{Dt}\dot{q}_d + K_{Pt}q_d + \tau_i \| \rfloor$$

The following conditions are obtained from the agreement of *Lemma 1*:

$$2\sqrt{\alpha_{t2}\alpha_{t1}} > \frac{\Delta_0\alpha_{t1}^2 + \alpha_{t2}\Delta_d\bar{\lambda}_{K_{Pt}}}{\underline{\lambda}_{K_{Pt}}\sqrt{\lambda_{\Gamma+K_{Dt}}}} \tag{15}$$

Based on the constraint (15), there always exist arbitrarily small new constants ($\beta_{tj|j=1..4}$) that simplify the inequality (14) as follows:

$$\begin{aligned}\dot{L} &\le -\beta_{t1}\|\dot{q}\|^4 - \beta_{t2}\|q\|^2\|\dot{q}\|^2 - \beta_{t3}\|\dot{q}\|^2 - \beta_{t4}\|q\|^2 \\ &\quad + \|\dot{q}\|\,\Delta_d\,(1+\alpha_{t2}\alpha_{t3}) + \alpha_{t1}\,\|q\|\,\Delta_d \\ &\le -\beta_{t1}\|\dot{q}\|^4 - \|\dot{q}\|\,(\beta_{t3}\,\|\dot{q}\| - \Delta_d\,(1+\alpha_{t2}\alpha_{t3})) \\ &\quad - \beta_{t2}\|q\|^2\|\dot{q}\|^2 - \|q\|\,(\beta_{t4}\,\|q\| - \Delta_d\alpha_{t1})\end{aligned} \tag{16}$$

Note that the term Δ_d is bounded. The result (16) implies that the system outputs $(q, \dot{q})$ are bounded. *Theorem 1* has thus been proven. ⊓

Remark 3: Working under the time-based PD control law (7), the closed-loop system is bounded stable with any positive-definite control gains K_{Dt} and K_{Pt}. However, the control accuracy needs to be further investigated.

Here, we define an indirect control objective:

$$\varepsilon = \dot{e} + K_i e \tag{17}$$

where $K_i = K_{Dt}^{-1}K_{Pt}$ is a positive-definite control gain matrix. In previous work, the new control objective (17) was normally called as a sliding-mode manifold [18], [51], [52].

The dynamics (1) could be re-expressed in terms of the new composited variable (17) in scope of an iterative axis:

$$M_i\dot{\varepsilon}_i = -C_i\varepsilon_i + \tau_i - d_i \tag{18}$$

where d_i is the lumped disturbance of the system in iteration i, that includes the model deviation and external disturbances:

$$d_i = M_i\,(\ddot{q}_d - K_i\dot{e}_i) + C_i\,(\dot{q}_d - K_i e_i) + g_i - f_i - \tau_{di} \tag{19}$$

Note that under the virtue of the control rule (6)-(7), the disturbance d_i is bounded. We can achieve the following statement for the control accuracy of the closed-loop system.

Corollary 1: The steady-state control error of the time-based control system in *Theorem 1* approaches to the following range:

$$e_{ss} = \lim_{t\to\infty}\left(K_{Pt}^{-1}\,(d_i - \tau_i)\right) \tag{20}$$

Its proof could be referred from previous work [22], [38], [41]. ⊓

Remark 4: The control error could be reduced by selecting large control gain K_{Pt}. However, to reach outstanding control outcomes, the uncertain nonlinearities and external disturbances in the system model must be eliminated. For this purpose, possible directions are adoption of robust adaptive nonlinear controllers [17], [21], [48] or high-gain observers [17], [53], [54]. Interestingly, the dynamical behaviors of the system would be recorded in the previous iteration data [23], [34]. By properly exploiting such data, it could result in surprising control achievement.

B. NEURAL ITERATIVE LEARNING CONTROL SIGNAL

In this subsection, an intelligent iterative-based control signal is going to be developed for a high-accuracy tracking control outcome using repetitive control behaviors and advantages of the ILC technology.

Inspired but different from previous studies [41], [55], [56], the iterative control rule is designed as

$$\tau_i = P_i\tau_{i-1} + \xi_i \tag{21}$$

where $P_i = diag\,\lfloor p_i \rfloor$ is a diagonal matrix of inheritance functions, and ξ_i is an excitation function.

As also reported in the past work, the iterative disturbance d_i was assumed to be no change on the iterative direction, and the iterative-based functions were chosen as

$$\begin{cases} P_i = Q\,\lfloor \varepsilon_i \rfloor \\ \xi_i = Q\,\lfloor \varepsilon_i \rfloor\, h\,\lfloor \varepsilon_i/\varepsilon_{i-1} \rfloor \end{cases} \tag{22}$$

in which, $Q\,\lfloor \varepsilon_i \rfloor$ is normally a filter function that is used to isolate unexpected disturbances from the iteration loop, while $h\,\lfloor \varepsilon_i/\varepsilon_{i-1} \rfloor$ could be simple functions or model-based adaptation functions or neural network models of either the previous or current iteration with time lifting [23], [35], [38], [55]. With such design, the iterative control signal has tended to completely believe either on the past control experiences or only on current iteration. Much research in the human society show that this action is not an appropriate choice in complicated situations [57], [58]. Hence, in this paper, a new intelligent ILC design is provided to deal with the aforeanalyzed problem.

Note that *Corollary 1* implies that once the iterative control signal τ_i approaches to the disturbance d_i, the control error will converge to zero or as small as possible. Hence, it is worth defining a new error:

$$\varsigma_i = \tau_i - d_i \tag{23}$$

By recalling the general control rule (21), variation of the new error (23) on the iteration axis is expressed as

$$\varsigma_i = P_i\varsigma_{i-1} + \xi_i - \varphi_{i,i-1} \tag{24}$$

where $\varphi_{i,i-1}$ is called as the iterative disturbance, that is formulated as:

$$\varphi_{i,i-1} = d_i - P_i d_{i-1} \tag{25}$$

The model (25) indicates that the new disturbance $\varphi_{i,i-1}$ contains both the present and past states on both the time and iterative axes. It can be easily observed that the disturbance d_i will approach to d_{i-1} once e_i approaches to e_{i-1}. Based on the aforementioned observation, the inheritance function could be selected as

$$p_{i,k|k=1..n} = \left(1 - e^{-\gamma_{i,p1,k}t}\right)e^{-\gamma_{i,p2,k}\varepsilon_{i,k}^2} \tag{26}$$

where $\gamma_{i,p1,k}$, $\gamma_{i,p2,k}$ are preselected positive constants.

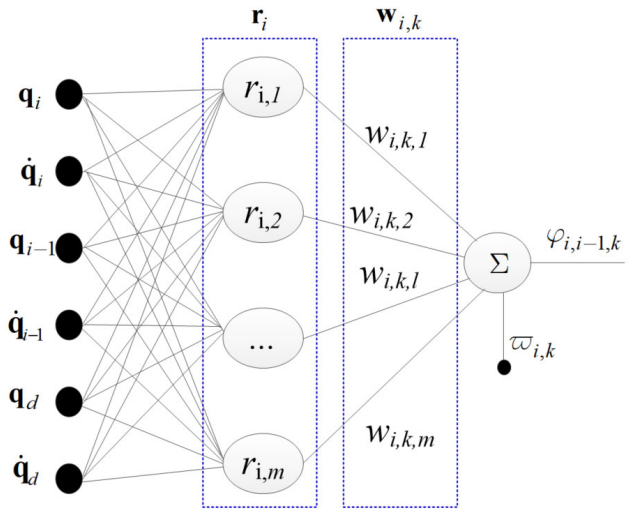

FIGURE 1. Structure of the employed neural network.

To design the excitation function, we can begin with approximating the new disturbance $\varphi_{i,i-1}$ as in (27) using universal approximation natures of neural networks [14], [17], [59]:

$$\varphi_{i,i-1,k|k=1..n} = w_{i,k}^T r_i \lfloor q_i, \dot{q}_i, q_{i-1}, \dot{q}_{i-1}, q_d, \dot{q}_d \rfloor + \varpi_{i,k} \tag{27}$$

where $w_{i,k} \in \Re^m$ is an optimal weight vector, $r_i \in \Re^m$ is a bounded regression vector, m is a selected length, and $\varpi_{i,k}$ is an approximation error. Structure of the network is illustrated in **Fig. 1**.

Note that the excitation function ξ_i is employed to compensate for the new disturbance $\varphi_{i,i-1}$. Therefore, it is designed as

$$\xi_{i,k|k=1..n} = \hat{w}_{i,k}^T r_i \lfloor q_i, \dot{q}_i, q_{i-1}, \dot{q}_{i-1}, q_d, \dot{q}_d \rfloor \tag{28}$$

where $\hat{w}_{i,k}$ is estimate of the vector $w_{i,k}$.

By adopting the model (27) and the selection (28) to the variation (24), we have

$$\varsigma_{i,k|k=1..n} = p_i \varsigma_{i-1,k} + \tilde{w}_{i,k}^T r_i - \varpi_{i,k} \tag{29}$$

where $\tilde{w}_{i,k} = \hat{w}_{i,k} - w_{i,k}$ is an estimation error.

The element-wise dynamics (29) reveal that the iterative control outcome totally depends on the learning of the excitation function. Thus, we design the following second-order adaptation law:

$$\hat{w}_{i,k|k=1..n} = \gamma_{i,w1,k}\hat{w}_{i-1,k} + \gamma_{i,w2,k}\hat{w}_{i-2,k} - \beta_{i,k}\frac{r_i \tanh\lfloor \varepsilon_{i,k} \rfloor}{1 + r_i^T r_i} \tag{30}$$

where $\beta_{i,k|k=1..n}$ are positive constants, and $\gamma_{i,w1,k|k=1..n}$, $\gamma_{i,w2,k|k=1..n}$ are learning rates.

So far, the novel ILC design seems to possess the model-free and adaptive features required. Its robustness is now discussed from the following investigations.

Lemma 2: For any bounded iterative disturbance that is expressed in a linear combination as presented in (27), the estimation error $\tilde{w}_{i,k}$ is bounded if the nonlinear learning rule (30) is employed with the learning rates complying with the constraint (31):

$$\begin{cases} 0 < |\gamma_{i,w1,k}| < 1 \\ 0 \le |\gamma_{i,w2,k}| < 1 \\ |\gamma_{i,w1,k}| + |\gamma_{i,w2,k}| < 1 \\ \gamma_{i,w2,k} \ge -0.25\gamma_{i,w1,k}^2 \end{cases} \tag{31}$$

Proof:

Variation of the estimation error on the iterative axis is described as in (32) by using the adaptation rule (30):

$$\begin{aligned} \tilde{w}_{i,k|k=1..n} = {} & \gamma_{i,w1,k}\tilde{w}_{i-1,k} + \gamma_{i,w2,k}\tilde{w}_{i-2,k} - w_{i,k} \\ & + \gamma_{i,w1,k}w_{i-1,k} + \gamma_{i,w2,k}w_{i-2,k} \\ & - \beta_{i,k}\frac{r_i \tanh\lfloor \varepsilon_{i,k} \rfloor}{1 + r_i^T r_i} \end{aligned} \tag{32}$$

The condition (31) could result in new inequalities:

$$\begin{cases} \gamma_{i,w2,k} < 1 + \gamma_{i,w1,k} \\ \gamma_{i,w2,k} < 1 - \gamma_{i,w1,k} \\ \gamma_{i,w2,k} \ge -0.25\gamma_{i,w1,k}^2 \end{cases} \tag{33}$$

Based on the constraints (31) and (33), it is always possible to separate the learning rates $(\gamma_{i,w1,k},\ \gamma_{i,w2,k})$ into the following interesting terms:

$$\begin{cases} \sigma_{i,w1,k}\sigma_{i,w2,k} = \gamma_{i,w2,k} \\ \sigma_{i,w1,k} - \sigma_{i,w2,k} = \gamma_{i,w1,k} \\ \sigma_{i,w1,k} = 0.5(\sqrt{\gamma_{i,w1,k}{}^2 + 4\gamma_{i,w2,k}} + \gamma_{i,w1,k}) < 1 \\ \sigma_{i,w1,k} = 0.5(\sqrt{\gamma_{i,w1,k}{}^2 + 4\gamma_{i,w2,k}} - \gamma_{i,w1,k}) < 1 \end{cases} \tag{34}$$

We next define a new composited estimation error:

$$v_{i,k|k=1..n} = \tilde{w}_{i,k} + \sigma_{i,w2,k}\tilde{w}_{i-1,k} \tag{35}$$

The variation (32) could be shortened as

$$\begin{aligned} v_{i,k|k=1..n} = {} & \sigma_{i,w1,k}v_{i-1,k} - w_{i,k} + \gamma_{i,w1,k}w_{i-1,k} \\ & + \gamma_{i,w2,k}w_{i-2,k} - \beta_{i,k}\frac{r_i \tanh\lfloor \varepsilon_{i,k} \rfloor}{1 + r_i^T r_i} \end{aligned} \tag{36}$$

By applying the triangle inequality [47], [56] to (36), the following regression series constraint is resulted in

$$\begin{aligned} \|v_{i,k|k=1..n}\| &\le |\sigma_{i,w1,k}|\,\|v_{i-1,k}\| + 2\bar{w}_{i,k} + \beta_{i,k} \\ &\le \ldots \le |\sigma_{i,w1,k}|^i\,\|v_{0,k}\| \\ &\quad + (2\bar{w}_{i,k} + \beta_{i,k})\frac{1 - |\sigma_{i,w1,k}|^{i-1}}{1 - |\sigma_{i,w1,k}|} \end{aligned} \tag{37}$$

From (37) and *Theorem 1*, it can be seen that the intermediate estimation error $(v_{i,k|k=1..n})$ is bounded. Applying the same

manner to the former estimation error ($\tilde{w}_{i,k}$) leads to

$$\begin{aligned}
&\left\|\tilde{w}_{i,k|k=1..n}\right\| \\
&\quad \le |\sigma_{i,w2,k}| \left\|\tilde{w}_{i-1,k}\right\| + \left\|v_{0,k}\right\| \\
&\qquad + \left(2\bar{w}_{i,k} + \beta_{i,k}\right) \frac{1-|\sigma_{i,w1,k}|^{i-1}}{1-|\sigma_{i,w1,k}|} \\
&\quad \le \ldots \le |\sigma_{i,w2,k}|^{i} \left\|\tilde{w}_{0,k}\right\| + \left\|v_{0,k}\right\| \frac{1-|\sigma_{i,w2,k}|^{i-1}}{1-|\sigma_{i,w2,k}|} \\
&\qquad + \left(2\bar{w}_{i,k} + \beta_{i,k}\right) \frac{1-|\sigma_{i,w1,k}|^{i-1}}{1-|\sigma_{i,w1,k}|} \frac{1-|\sigma_{i,w2,k}|^{i-1}}{1-|\sigma_{i,w2,k}|}
\end{aligned} \tag{38}$$

This result indicates that the estimation error ($\tilde{w}_{i,k}$) is bounded, and *Lemma 2* has been thus proven. □

Theorem 2: If the iterative disturbance (25) is bounded and the iterative control signal is updated by the rules (21), (26), (28), (30) and (31), variation of the iterative error (23) is stable.

Proof:

By using (27)-(28), the variation (24) is simplified in an element-wise form

$$\varsigma_{i,k|k=1..n} = p_{i,k}\varsigma_{i-1,k} + \tilde{w}_{i,k}^{T} r_i - \varpi_{i,k} \tag{39}$$

In cases of the non-zero indirect control objectives ($\varepsilon_{i,k} \neq 0$), the inheritance function is less than one ($p_{i,k} < 1$). Using the triangle inequality for the variation (39), one has

$$\begin{aligned}
|\varsigma_i| &\le \rho|\varsigma_{i-1}| + |\bar{\tilde{w}}_{i,k}^{T} r_i| + |\bar{\varpi}_{i,k}| \\
&\le \ldots \le \rho^{i}|\varsigma_{i-1}| + \frac{1-\rho^{i-1}}{1-\rho}(|\bar{\tilde{w}}_{i,k}^{T} r_i| + |\bar{\varpi}_{i,k}|)
\end{aligned} \tag{40}$$

where ($p_{i,k} \le \rho < 1$) is an upper bounds of $p_{i,k}$.

From the result of *Lemma 2*, the estimation error ($\tilde{w}_{i,k|k=1..n}$) is bounded, hence the iterative error ς_i is bounded. From (21), (26) and (28), or (23), the iterative control signal ($\tau_{i,k|k=1..n}$) is bounded as well.

In cases of the perfect indirect control error ($\varepsilon_{i,k} = 0$), the inheritance function is equal to one ($p_{i,k} = 1$). By noting (28)-(30), the control law (21) could be rewritten as

$$\tau_{i,k|k=1..n} = \tau_{i-1,k} + \gamma_{w1,k}\hat{w}_{i-1,k}^{T} r_i + \gamma_{w2,k}\hat{w}_{i-2,k}^{T} r_i \tag{41}$$

Applying the same triangle inequality, we have

$$\begin{aligned}
|\tau_{i,k|k=1..n}| &\le |\tau_{i-1,k}| + \left(|\gamma_{w1,k}| + |\gamma_{w2,k}|\right) c_{i0} \\
&\le \ldots \le |\tau_0(k)| + \frac{1-\left(|\gamma_{w1,k}| + |\gamma_{w2,k}|\right)^{i}}{1-|\gamma_{w1,k}| - |\gamma_{w2,k}|} c_{i0}
\end{aligned} \tag{42}$$

where $c_{i0} = \max\left\lfloor |\hat{w}_{i,k}|^{T} |r_i| \right\rfloor$ denotes an upper bound of the estimated iterative disturbance, $\tau_0(k)$ is an iterative control value at the last moment of the imperfect indirect control case.

From yield of *Lemma 2* with the condition (31), at which the upper bound of $\bar{\hat{w}}_{i-1,k}$ is confirmed, and from the virtue of the imperfect cases where $\tau_0(k)$ is bounded, the inequality (42) implies that the iterative control torque in the perfect case is bounded. It leads the boundedness of the iterative error in (23). The proof of *Theorem 2* has thus been completed. □

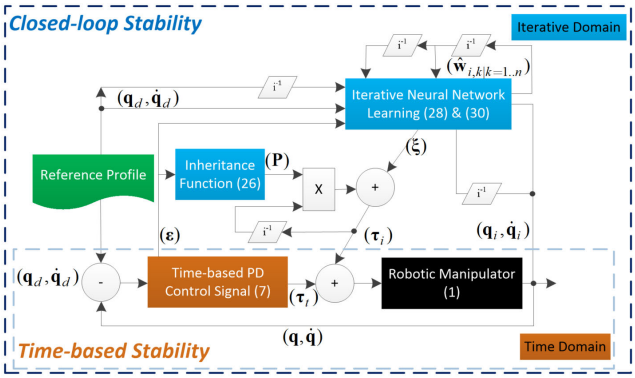

FIGURE 2. Block diagram of the proposed controller.

Remark 5: Overview of the proposed control approach is illustrated in **Fig. 2**. The general robotic system (1) itself is an unstable plant with complicated nonlinear uncertain dynamics and affected by external disturbances [13], [34]. In the proposed control strategy, the PD control signal (7) is first used to stabilize internal/external dynamics, and the new neural ILC terms ((26), (28), and (30)) are then integrated to provide expected control performances. In fact, to obtain an excellent control error (5), one could employ various neural networks [14], [15], [16], [17] to learn the disturbance (19) using current states of the system (1). As presented in (27), the regression vector of the iterative-based neural network contains more states than that of the time-based neural networks. Hence, by using the PDISN technique, one could utilize the control experiences in the past to result in higher control performances.

Remark 6: With the iterative-based control design, the convergence of the control performance (24) is accomplished in a spiral manner. In cases of the large indirect control error (17), the inheritance function becomes small, and the convergence process is mainly based on the learning of the excitation process (28), (30). It means that in this case the controller reduces the creditability of the past control experience and mainly uses state information of two consecutive latest iterations to generate the iterative control signal. As proven in *Lemma 2*, the network could well learn the iterative disturbance in several steps. The errors (23) as well as (17) would then converge to a smaller bound. As a sequence, the bound of the iterative disturbance (25) would be reduced due to its special properties on the iteration axis [23], [44]. This fact makes the error (23) continuously smaller, even though the inheritance function approaches to one. Note also that in this situation, the excitation function ξ_i will become smaller as well, and the controller has a good reason to believe on the previous control experiences. Comparing to almost previous studies [37], [38], [41] that completely put the iterative control mission on one certain iteration (current or past) shoulder, the proposed iterative method seems more flexible in technical viewpoint and closely to human thinking.

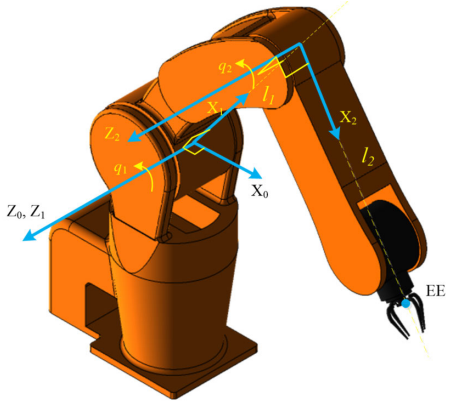

FIGURE 3. Configuration of the simulation robot.

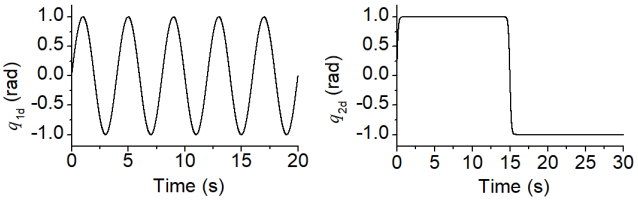

FIGURE 4. Desired trajectories of the robot joints in the first simulation.

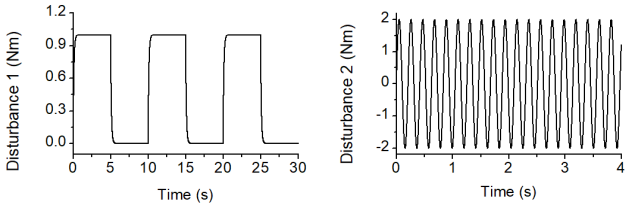

FIGURE 5. External disturbances affecting to the robot joints in the first simulation.

Remark 7: Initial resetting conditions are crucial issues with conventional ILC techniques [38], [45]. With the flexible learning rules (21), (26), (28), (30) and proven by *Lemma 2* and *Theorem 2*, the robustness of the closed-loop system could be confirmed over such problems.

Remark 8: To approximate the iterative disturbance (25), ones could employ many types of nonlinear neural networks such as deep neural networks or large-size encoded two-layer neural networks [9], [11], [66]. The deep networks have been shown outstanding learning performances in a wide variety of applications, but the learning processes are commonly slow due to attrition of learning signals transferred throughout many layers [63], [65]. They would be thus great with offline-learning systems [62], [67]. On the other side, in the functional two-layer networks, the first layer works as a feature-extracting module, and the second layer is then optimized by learning algorithms to result in desired approximation precision [6], [10]. Thanks to the fast adaptation and low computation, they are suitable for automatic intelligent control systems that require online learning ability [9], [10], [62], [63].

Remark 9: Under the approximation structure (27), (28) or the graphical presentation in **Fig. 1**, if the regression vector (r_i) can be able to capture all features of the input signals inside their working ranges, a larger length (m) of the vector (r_i) would result in a smaller bound of the approximation error $\varpi_{i,k}$ [63], [64]. A trade-off value of the length (m) to ensure a good transient iterative performance and a proper volume of the controller memory has to be considered carefully.

Remark 10: From (30), it can be seen that the learning process of the neural network (27), (28) is activated by the indirect control error (ε) in (17). As also reflected from (24), once the error (ε) converges to zero, the iterative disturbance $(\varphi_{i,i-1})$ converges to zero as well. At that time, if all elements of the regression vector (r_i) are normalized in a range of (0; 1], the estimation weight vectors $\hat{w}_{i,k|k=1..n}$ tend to converge to zero. The smallest possible absolute values of the indirect control error (ε) and of all elements of the estimation weight vectors $(\hat{w}_{i,k|k=1..n})$ can confim the working effectiveness of the neural network designed and the new ILC approach proposed.

IV. VERIFICATION RESULTS

In this section, the effectiveness of the proposed controller is further discussed based on validation results achieved in a simulation environment.

A. SETUP

To evaluate the control performances of the PDISN controller, comparative simulations were carried out on a 2-DOF robot [28], as sketched in **Fig. 3**. The robot dynamics were derived from previous work [13], [16]:

$$
\begin{aligned}
M\lfloor q\rfloor &= \begin{bmatrix} m_{11} & m_2 l_2^2 + l_1 l_2 m_2 \cos(q_2) \\ m_2 l_2^2 + l_1 l_2 m_2 \cos(q_2) & m_2 l_2^2 \end{bmatrix} \\
m_{11} &= m_2 l_2^2 + 2 l_1 l_2 m_2 \cos(q_2) + (m_1 + m_2) l_1^2 \\
C\lfloor q, \dot{q}\rfloor \dot{q} &= \begin{bmatrix} -m_2 l_1 l_2 \sin(q_2)\dot{q}_2\,(\dot{q}_2 + 2\dot{q}_1) \\ m_2 l_1 l_2 \sin(q_2)\dot{q}_1^2 \end{bmatrix} \\
g\lfloor q\rfloor &= \begin{bmatrix} m_2 l_2 g \cos(q_1 + q_2) + (m_1 + m_2)\, l_1 g \cos(q_1) \\ m_2 l_2 g \cos(q_1 + q_2) \end{bmatrix} \\
f\lfloor \dot{q}\rfloor &= \begin{bmatrix} a_1 \dot{q}_1 \\ a_2 \dot{q}_2 \end{bmatrix}
\end{aligned}
$$

where $q_{1,2}$ are joint positions, and m_i, $l_{i|i=1,2}$ are masses and lengths of the robot links, respectively. The system parameters were selected to be $l_1 = 0.2, l_2 = 0.3, m_1 = 2, m_2 = 0.5, a_1 = a_2 = 2$.

In the simulations, the learning and control gains of the proposed controller were chosen to be:

$$
\begin{cases}
K_{Pt} = 30 I_2; K_{Dt} = 2 I_2; \beta_{i,1} = \beta_{i,2} = 2; \\
\gamma_{i,p1,1} = \gamma_{i,p1,2} = 20; \gamma_{i,p2,1} = \gamma_{i,p2,2} = 0.005; \\
\gamma_{i,w1,1} = \gamma_{i,w1,2} = 0.2; \gamma_{i,w2,1} = \gamma_{i,w2,2} = 0.01.
\end{cases}
$$

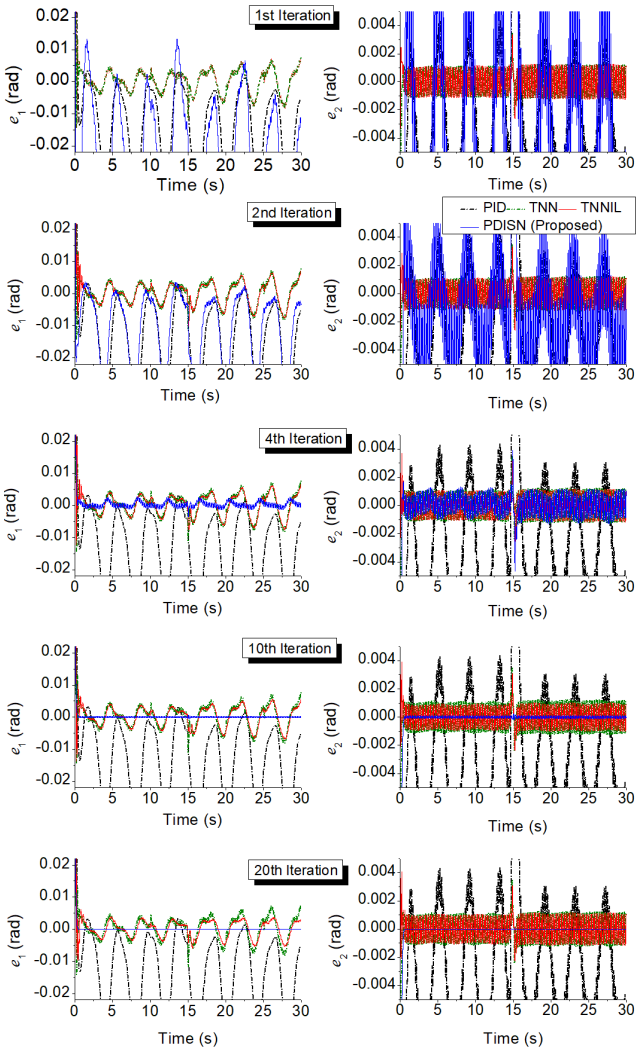

FIGURE 6. Control errors of the investigating systems on the time axis and the iteration axis in the first simulation.

The regression vector (r_i) of the neural network was built up from 729 neurons using *logsig* functions. To clearly validate the advantages of the proposed ILC method, a conventional PID controller [1], Time-based Neural-Network (TNN) controller [60], and Time-based Neural-Network Iterative Learning (TNNIL) controller [41] were deployed to control the same system in same working conditions. Parameters of the PID controller were selected as follows:

$$K_P = diag([250;\ 200]);\ K_I = 3I_2;\ K_D = 50I_2;$$

The TNN controller was resued from previous work [60] with the following design:

$$\begin{cases} e_{TNN} = q_d - q; \\ r_{TNN} = \dot{e}_{TNN} + \Lambda_{TNN} e_{TNN}; \\ \tau_{TNN} = K_{v,TNN} r_{TNN} \\ \qquad + \hat{W}_{TNN}^T \phi_{TNN} \lfloor e_{TNN}, \dot{e}_{TNN}, q_d,\ \dot{q}_d, \ddot{q}_d \rfloor; \\ \dot{\hat{W}}_{TNN} = \sigma_{TNN} \phi_{TNN} \lfloor e_{TNN}, \dot{e}_{TNN}, q_d,\ \dot{q}_d, \ddot{q}_d \rfloor r_{TNN}^T; \end{cases}$$

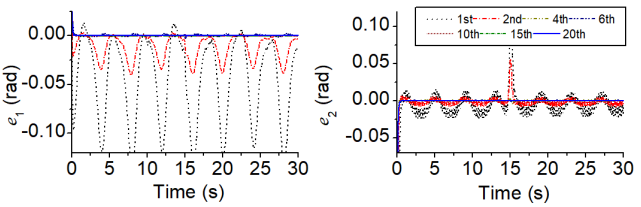

FIGURE 7. Control errors of the proposed controller on the time axis and the iteration axis in this first simulation.

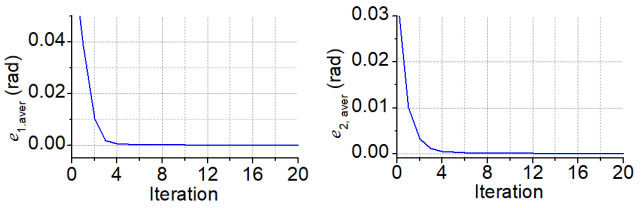

FIGURE 8. Average absolute control errors of the proposed controller on the iteration axis in the first simulation.

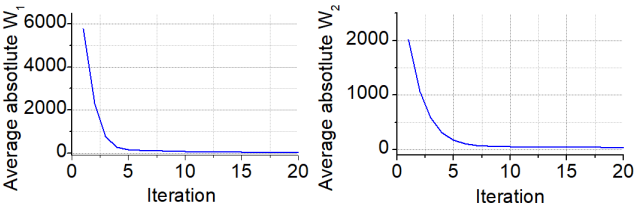

FIGURE 9. Average absolute values of the weight vectors learnt by the proposed algorithm in the first simulation.

where $\phi_{TNN} \lfloor e_{TNN}, \dot{e}_{TNN}, q_d,\ \dot{q}_d, \ddot{q}_d \rfloor$ was a regression vector of *logsig* functions, other control and learning gains were obtained by a manual method, as follows: $\Lambda_{TNN} = 15I_2$; $K_{v,TNN} = 2I_2$; $\sigma_{TNN} = 100$.

The TNNIL controller was extended from another previous study [41]. Its detailed design was as

$$\begin{cases} e_{IC} = q - q_d; \\ z_{IC} = \dot{e}_{IC} + a_{IC} e_{IC}; \\ \tau_{IC} = \tau_{f,IC} + \tau_{c,IC} + \tau_{l,IC}; \\ \tau_{f,IC} = L_{IC} z_{IC}; \\ \tau_{l,i+1,IC} =^i \tau_{l,i,IC} + \beta_{IC} L_{IC} z_{i,IC}; \\ \tau_{c,IC} = \hat{W}_{IC}^T \phi_{IC} \lfloor q, \dot{q}, q_d,\ \dot{q}_d, \ddot{q}_d \rfloor; \\ \dot{\hat{W}}_{IC} = \sigma_{IC} \phi_{IC} \lfloor q, \dot{q}, q_d,\ \dot{q}_d, \ddot{q}_d \rfloor z_{IC}^T; \\ \hat{W}_{i+1,IC} \lfloor 0 \rfloor = \hat{W}_{i,IC} \lfloor T \rfloor \end{cases}$$

where $\phi_{IC} \lfloor q, \dot{q}, q_d,\ \dot{q}_d, \ddot{q}_d \rfloor$ was also a regression vector of *logsig* functions, and T is the duration of each iteration. The control and learning gains of the TNNIL controller were chosen as: $a_{IC} = 15$; $L_{IC} = 2I_2$; $\beta_{IC} = 0.5$; $\sigma_{IC} = 100$.

B. SIMULATION RESULTS

In the first simulation, sinusoidal ($q_{1d} = sin(0.4\pi t)(rad)$) and multi-step ($q_{2d} = ((1 - e^{-10t})/(1 + e^{-10t})) - 2e^{10(t-15)}/(1 + e^{10(t-15)})$) signals, as shown in **Fig. 4**,

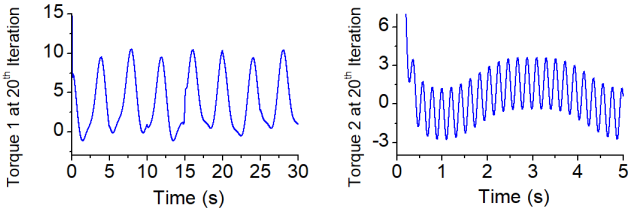

FIGURE 10. Control signals of the proposed controller at the 20^{th} iteration in the first simulation.

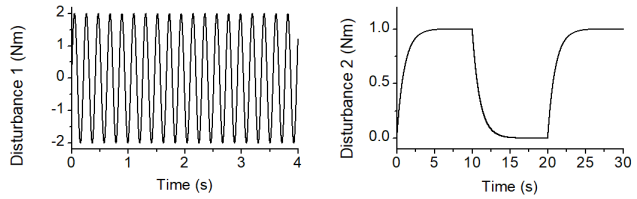

FIGURE 11. External disturbances affecting to the robot joints in the second simulation.

were selected as reference trajectories of joints 1 and 2, respectively. The initial joint positions were chosen to be 0.2 (rad) and −0.15 (rad). External disturbances of the system dynamics (1) were chosen as presented in **Fig. 5**. The four controllers were applied to control the robot, and their control results obtained in 20 iterations are plotted in **Figs. 6– 10**.

As shown in **Fig. 6**, the well-tuned PID controller could stabilize the system outputs in good control accuracies: 0.038 (rad) for the sinusoidal trajectory and 0.012 (rad) for the step trajectory under the large external disturbances. The control accuracies could be increased by employing adaptation natures of the neural networks to learn the system behaviors on the time axis. As seen in **Fig. 6**, the neural controllers always delivered higher control performances than the PID one. Control precision of the TNN approach was clearly improved: the control errors at the first and second joints were 0.0032 (rad) and 0.0012 (rad), respectively. Furthermore, if the system operated in a repetitive fashion, iterative-based control methods could be applied for higher control efficiency. **Fig. 6** also reveals that composition of a time-based neural-network control signal and a conventional ILC term in the TNNIL method could attenuate the perturbance more effectively and yielded promising control results: after 20 iterations, the control errors at the first and second joints were 0.0025 (rad) and 0.0009 (rad), respectively. In fact, the enhancement of the control performance was just minor by using the previous iterative learning control scheme in this case. As an innovative step, in this paper, we propose the new intelligent iterative high-order control framework as clearly discussed in *Section III*. Its control effect has been illustrated throughout the control outcomes obtained and shown in **Figs. 6 - 10**. As depicted in **Fig. 6**, in the first iteration, since the proposed control signal was just generated

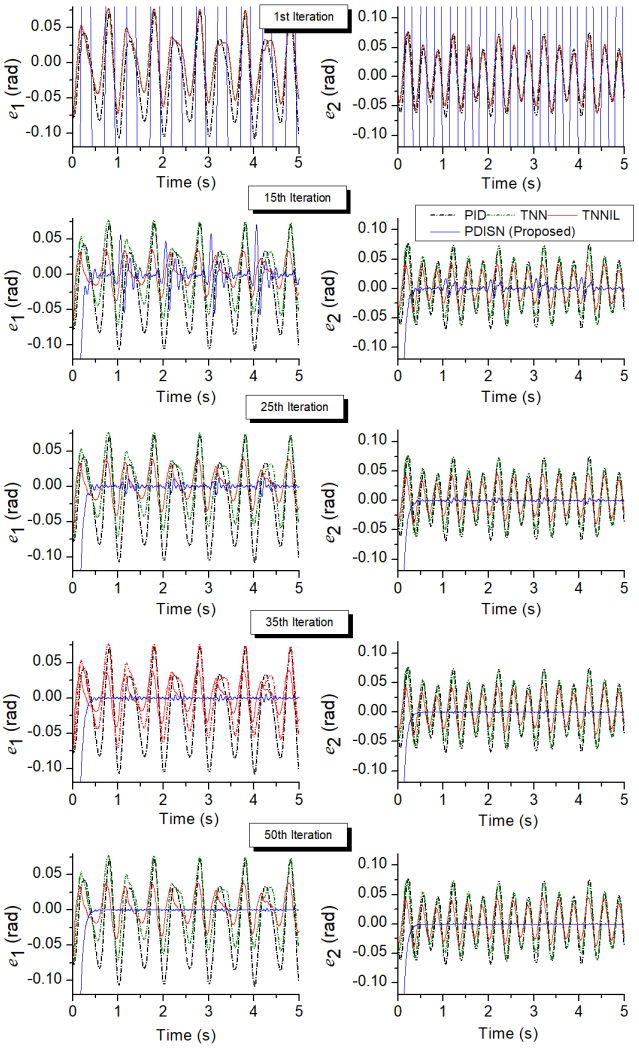

FIGURE 12. Control errors of the investigating systems on the time axis and the iteration axis in the second simulation.

by a poor PD control engine and the intelligent ILC was not applied at all, the control performance of the designed control approach looked even worse than that of the well-tuned PID one. In the second iteration, at which the new ILC framework had been gone into operation, the control performances seemed to be improved, but still not higher than those of the others, especially at the second joint that was suffered by the harsh external disturbance. However, learnability of the proposed control approach for this robotic system could be observed as comparing data of the two iterations. After completing 20 iterations of working, the PDISN controller surprisingly delivered the best control results under the severe working condition: the control errors at the first and second joints reached to 5.4×10^{-6} (rad) and 2.1×10^{-6} (rad), respectively. The learning ability of the PDISN method can be observed more clearly by different forms of the control errors presented in **Figs. 7** and **8**. The data indicate that the PDISN

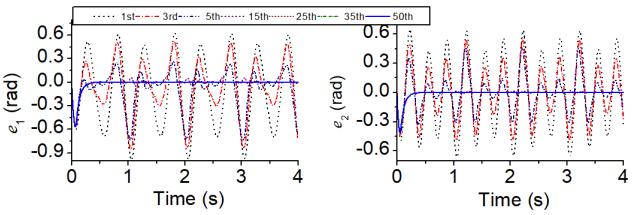

FIGURE 13. Control errors of the proposed controller on the time axis and the iteration axis in this second simulation.

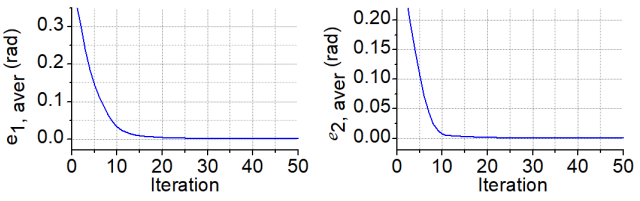

FIGURE 14. Average absolute control errors of the proposed controller on the iteration axis in the second simulation.

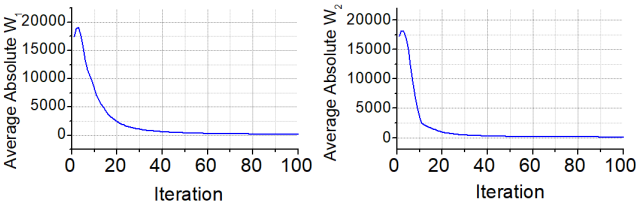

FIGURE 15. Average absolute values of the weight vectors learnt by the proposed algorithm in the second simulation.

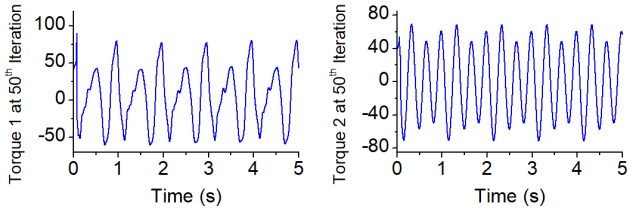

FIGURE 16. Control signals of the proposed controller at the 50^{th} iteration in the second simulation.

technique worked well with the robotic system in various conditions regardless of starting from a weak-performance level. **Fig. 9** presents the average absolute values of the neural weight vectors ($\hat{w}_{i,1}$ and $\hat{w}_{i,2}$) learnt by the proposed control algorithm on the iteration axis. The convergence of these average values to zero satisfies the discussions in *Remark 10*. In addition, the control signals shown in **Fig. 10** indicate that the proposed iterative learning method could convincingly record information of both internal and external disturbances, and then compensate for them in the control phase to result in the excellent control performances with smooth control behaviors.

In the second simulation, the controllers were challenged in more draconic working conditions in which the desired

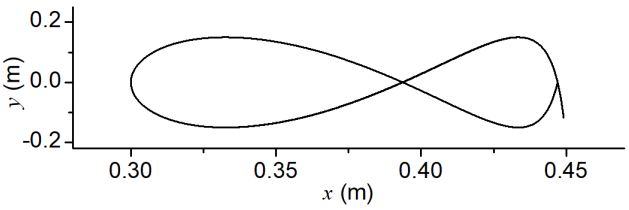

FIGURE 17. The desired end-effector trajectory of the robot in the third simulation.

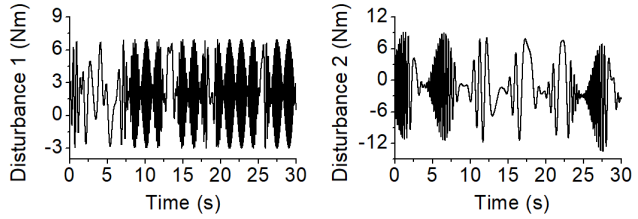

FIGURE 18. External disturbances affecting to the robot joints in the third simulation.

profiles were changed to be ($q_{1d} = sin(4\pi t)(rad)$ and $q_{2d} = sin(6\pi t)(rad)$), and the external disturbances affecting to the system were also reselected as shown in **Fig. 11**. After applying the same controllers to the system with the same initial joint values, new simulation results are presented in **Figs. 12-16**.

In the new operation conditions, as seen in **Fig. 12**, the PID and TNN controllers still maintained their robustness with acceptable control errors: 0.095 (rad) for the PID one and 0.07 (rad) for the TNN one at joint 1, for instance. The data in **Fig. 12** confirm the learning effectiveness of the TNNIL method: for example, the control accuracy after 50 iterations increased to 0.04 (rad) at joint 1, and the same behaviors could be seen in the control outcome of the joint 2. Even though supported by a strong time-based neural network control signal, the simulation results however reveal that the nonlinearities, uncertainties and disturbances were not completely terminated using the previous ILC one. We believe that such problems could be efficiently dealt with by the PDISN controller thanks to the proper neural-network-based design (21), (26), (28), (30) and (31). As demonstrated in detail in **Fig. 12** or in summarization modes in **Figs. 13** and **14**, the control performance of the proposed controller was improved from iteration to iteration: after 50 iterations, the steady-state control errors of joint 1 and 2 reached to good values of 0.00036 (rad) and 0.00015 (rad), respectively. Once the good control errors were released, all elements of the estimation weight vectors ($\hat{w}_{i,1}$ and $\hat{w}_{i,2}$) were converged to zero as shown in **Fig. 15** or as discussed in *Remark 10*. Furthermore, as illustrated in **Fig. 16**, control torques generated by the proposed method were still smooth through many iterations.

To verify the controllers with practical challenges, in the third simulation, the end-effector of the robot was controlled

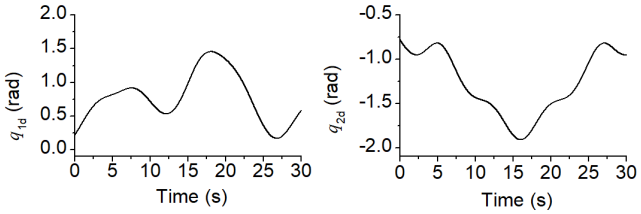

FIGURE 19. The desired trajectories of the robot joints in the third simulation.

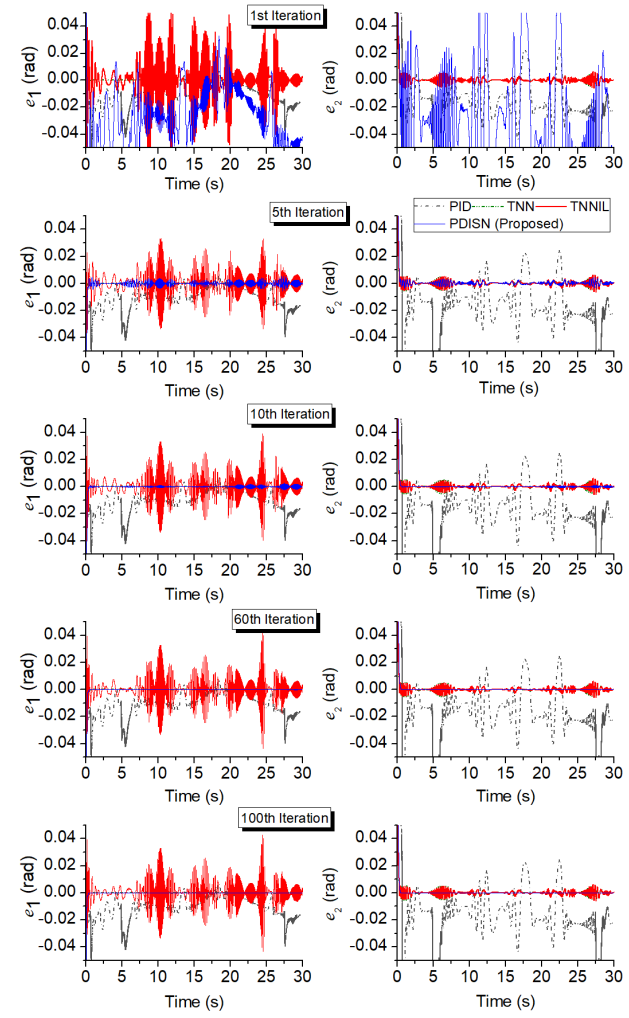

FIGURE 20. Control errors of the investigating systems on the time axis and the iteration axis in the third simulation.

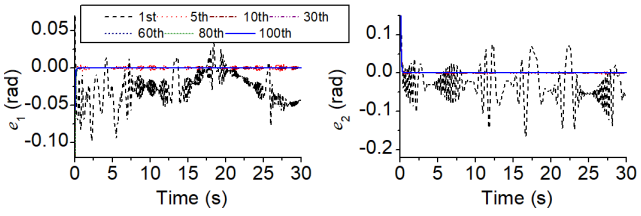

FIGURE 21. Control errors of the proposed controller on the time axis and the iteration axis in this third simulation.

to follow a certain trajectory, as depicted in **Fig. 17**, under very complicated disturbances, as shown in **Fig. 18**, that

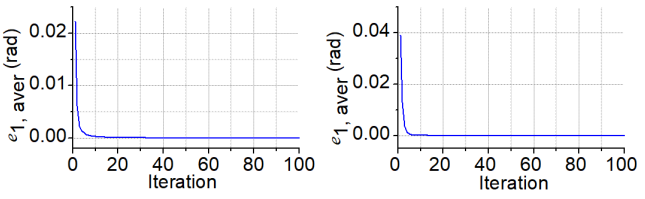

FIGURE 22. Average absolute control errors of the proposed controller on the iteration axis in the third simulation.

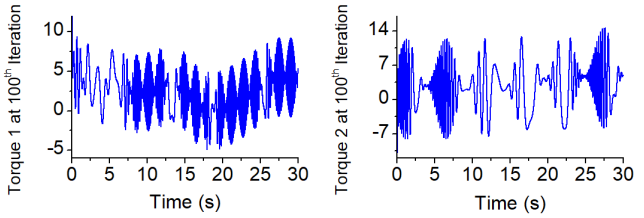

FIGURE 23. Control signals of the proposed controller at the 100th iteration in the third simulation.

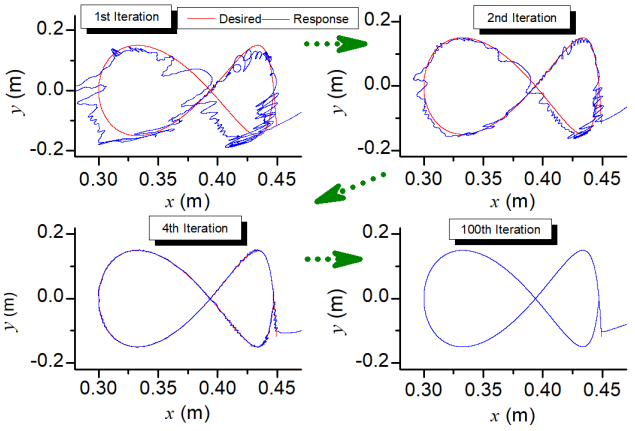

FIGURE 24. Responses of the proposed controllers in task-space view from iterations in the third simulation.

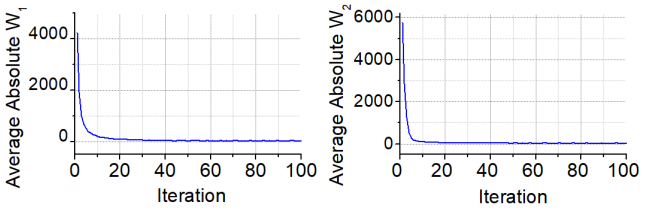

FIGURE 25. Average absolute values of the weight vectors learnt by the proposed algorithm in the third simulation.

seriously affected to joint motions. By applying proper inverse kinematics [13], the corresponding desired trajectories of the joint angles are plotted in **Fig. 19**. In this test, the initial values of the joint positions of the proposed controllers were set to be different for each iterations: $q_{1,ini}\lfloor i\rfloor = 0.2 + 0.2sin(i)$; $q_{2,ini}\lfloor i\rfloor = -0.15 + 0.2cos(i)$.

After applying the same controllers to the system in the same testing conditions, the obtained results are presented in **Figs. 20** - **25**. The data shown in **Fig. 20** once again strongly confirm the effectiveness and reliability of the proposed control algorithm in various working conditions. Although heavily affected by the sturdy external disturbances and the inconsistently initial joint positions, the control accuracies of the PDISN controller increased iteration-by-iteration to outstanding levels: as observed in **Figs. 20** - **22**, after 100th iteration, the control errors of joints 1 and 2 were about 1.2×10^{-7} (rad) and 10^{-7} (rad), respectively. Meanwhile, the best values of other comparative controllers in this test, as depicted in **Fig. 20**, were 0.02 (rad) and 0.006 (rad) for joints 1 and 2, respectively. By comparing **Figs. 18** and **23**, it can be seen that the proposed control algorithm could learn well the internal/external disturbances. The learning results were then adopted to eliminate the system dynamics in the control phase to result in the excellent tracking control outcomes, as shown in the joint-space view in **Figs. 20** - **22**, and, as demonstrated in the task-space view in **Fig. 24**. **Fig. 25** reveals that all elements of the weight vectors also well approached to zero but containing few vibrations. These variations were generated by the proposed controller in the transient time of each iteration to compensate for difference of the initial values of the joints. It means that the initial resetting problem facing in many classical ILC approaches was effectively treated by the PDISN one. Note that to achieve high control performances using this control approach, users do not need a complicated time-based control signals to support the iterative learning process. Hence, outperformances of the proposed controllers over the previous ones in terms of high precision, free initial conditions, robustness, adaptation and smooth control behaviors, can be confirmed throughout these validation results.

V. CONCLUSION

An efficient intelligent ILC method has been proposed for motion control of robotic manipulators. The controller is supported by a simple PD control signal in the time domain. The control performance is then enhanced by a learning control signal designed in the iteration domain. To cope with initial resetting problems as well as efficiently eliminate the time-iterative-based disturbances, the iterative signal is built up by a flexible inheritance term and an appropriate neural excitation structure. A special second-order learning law is derived for operation of the iterative network. Stability of the whole controller is thoroughly proven using Lyapunov-based analyses and regression series criteria. Effectiveness and reliability of the proposed control approach were carefully validated by intensive comparative simulation results. In the near future, the proposed controller will be improved with a structural learning algorithm to optimize computational time and be verified on real-time robotic manipulators. In practical operation, the desired joint trajectories are selected complying with the inertial nature of the verifying robot.

REFERENCES

[1] P. Rocco, "Stability of PID control for industrial robot arms," *IEEE Trans. Robot. Autom.*, vol. 12, no. 4, pp. 606–614, Aug. 1996.
[2] G. Michalos, J. Spiliotopoulos, S. Makris, and G. Chryssolouris, "A method for planning human robot shared tasks," *CIRP J. Manuf. Sci. Technol.*, vol. 22, pp. 76–90, Aug. 2018.
[3] Keenon Robotics. (2023). *Dinerbot T6*. [Online]. Available: https://www.keenonrobot.com/EN/index/Page/index/catid/7.html
[4] M. Foumani, I. Gunawan, K. Smith-Miles, and M. Y. Ibrahim, "Notes on feasibility and optimality conditions of small-scale multifunction robotic cell scheduling problems with pickup restrictions," *IEEE Trans. Ind. Informat.*, vol. 11, no. 3, pp. 821–829, Jun. 2015.
[5] ABB Cooperation, Industrial Robot Controllers. (2023). *ABB Value Provider Program*. [Online]. Available: https://new.abb.com/products/robotics/controllers
[6] W. Sun, Y. Wu, and X. Lv, "Adaptive neural network control for full-state constrained robotic manipulator with actuator saturation and time-varying delays," *IEEE Trans. Neural Netw. Learn. Syst.*, vol. 33, no. 8, pp. 3331–3342, Aug. 2022.
[7] Q. Guo, Y. Zhang, B. G. Celler, and S. W. Su, "Neural adaptive backstepping control of a robotic manipulator with prescribed performance constraint," *IEEE Trans. Neural Netw. Learn. Syst.*, vol. 30, no. 12, pp. 3572–3583, Dec. 2019.
[8] Y. Park, I. Jo, J. Lee, and J. Bae, "A dual-cable hand exoskeleton system for virtual reality," *Mechatronics*, vol. 49, pp. 177–186, Feb. 2018, doi: 10.1016/j.mechatronics.2017.12.008.
[9] M. Wang and A. Yang, "Dynamic learning from adaptive neural control of robot manipulators with prescribed performance," *IEEE Trans. Syst., Man, Cybern., Syst.*, vol. 47, no. 8, pp. 2244–2255, Aug. 2017.
[10] D. X. Ba, T. Q. Dinh, and K. K. Ahn, "An integrated intelligent nonlinear control method for a pneumatic artificial muscle," *IEEE/ASME Trans. Mechatronics*, vol. 21, no. 4, pp. 1835–1845, Aug. 2016.
[11] W. He, Y. Chen, and Z. Yin, "Adaptive neural network control of an uncertain robot with full-state constraints," *IEEE Trans. Cybern.*, vol. 46, no. 3, pp. 620–629, Mar. 2016.
[12] W.-H. Zhu, *Virtual Decomposition Control: Toward Hyper Degrees of Freedom Robots*. Berlin, Germany: Springer-Verlag, 2010.
[13] J. Craig, *Introduction to Robotics: Mechanics and Control*, 4th ed. Upper Saddle River, NJ, USA: Prentice-Hall, 2018.
[14] D. Xuan and J. Bae, "A precise neural-disturbance learning controller of constrained robotic manipulators," *IEEE Access*, vol. 9, pp. 50381–50390, 2021.
[15] M. Wang, Y. Zou, and C. Yang, "System transformation-based neural control for full-state-constrained pure-feedback systems via disturbance observer," *IEEE Trans. Cybern.*, vol. 52, no. 3, pp. 1479–1489, Mar. 2022, doi: 10.1109/TCYB.2020.2988897.
[16] L. Wu, Q. Yan, and J. Cai, "Neural network-based adaptive learning control for robot manipulators with arbitrary initial errors," *IEEE Access*, vol. 7, pp. 180194–180204, 2019.
[17] W. He, Y. Sun, Z. Yan, C. Yang, Z. Li, and O. Kaynak, "Disturbance observer-based neural network control of cooperative multiple manipulators with input saturation," *IEEE Trans. Neural Netw. Learn. Syst.*, vol. 31, no. 5, pp. 1735–1746, May 2020.
[18] M. Chen and S. S. Ge, "Adaptive neural output feedback control of uncertain nonlinear systems with unknown hysteresis using disturbance observer," *IEEE Trans. Ind. Electron.*, vol. 62, no. 12, pp. 7706–7716, Dec. 2015.
[19] M. Wang, Z. Wang, H. Dong, and Q. Han, "A novel framework for backstepping-based control of discrete-time strict-feedback nonlinear systems with multiplicative noises," *IEEE Trans. Autom. Control*, vol. 66, no. 4, pp. 1484–1496, Apr. 2021, doi: 10.1109/TAC.2020.2995576.
[20] F. Chao, D. Zhou, C. Lin, L. Yang, C. Zhou, and C. Shang, "Type-2 fuzzy hybrid controller network for robotic systems," *IEEE Trans. Cybern.*, vol. 50, no. 8, pp. 3778–3792, Aug. 2020.
[21] Z. Liu, G. Lai, Y. Zhang, and C. L.P. Chen, "Adaptive fuzzy tracking control of nonlinear time-delay systems with dead-zone output mechanism based on a novel smooth model," *IEEE Trans. Fuzzy Syst.*, vol. 23, no. 6, pp. 1998–2011, Dec. 2015, doi: 10.1109/TFUZZ.2015.2396075.

[22] T. Kuc and J. S. Lee, "An adaptive learning control of uncertain robotic systems," in *Proc. 30th IEEE Conf. Decis. Control*, Dec. 1991, pp. 1206–1211.
[23] D. A. Bristow, M. Tharayil, and A. G. Alleyne, "A survey of iterative learning control," *IEEE Control Syst. Mag.*, vol. 26, no. 3, pp. 96–114, Jun. 2006.
[24] M. Garden, "Learning control of actuators in control systems," U.S. Patent 3 555 252, Dec. 1, 1971.
[25] M. Uchiyama, "Formation of high-speed motion pattern of a mechanical arm by trial," *Trans. Soc. Instrum. Control Eng.*, vol. 14, no. 6, pp. 706–712, 1978.
[26] M. Takegaki and S. Arimoto, "A new feedback method for dynamic control of manipulators," *J. Dyn. Syst., Meas., Control*, vol. 103, no. 2, pp. 119–125, Jun. 1981.
[27] P. Bondi, G. Casalino, and L. Gambardella, "On the iterative learning control theory for robotic manipulators," *IEEE J. Robot. Autom.*, vol. 4, no. 1, pp. 14–22, Feb. 1988.
[28] S. Sivakumar. (2020). *A Conceptual Design Model of a 2 DOF Robot Arm*. [Online]. Available: https://grabcad.com/library/2-dof-robot-arm-1
[29] S. S. Saab, D. Shen, M. Orabi, D. Kors, and R. H. Jaafar, "Iterative learning control: Practical implementation and automation," *IEEE Trans. Ind. Electron.*, vol. 69, no. 2, pp. 1858–1866, Feb. 2022.
[30] S. He, W. Chen, D. Li, Y. Xi, Y. Xu, and P. Zheng, "Iterative learning control with data-driven-based compensation," *IEEE Trans. Cybern.*, vol. 52, no. 8, pp. 7492–7503, Aug. 2022.
[31] P. D. Nguyen and N. H. Nguyen, "An intelligent parameter determination approach in iterative learning control," *Eur. J. Control*, vol. 61, pp. 91–100, Sep. 2021.
[32] R. Mengacci, F. Angelini, M. G. Catalano, G. Grioli, A. Bicchi, and M. Garabini, "On the motion/stiffness decoupling property of articulated soft robots with application to model-free torque iterative learning control," *Int. J. Robot. Res.*, vol. 40, no. 1, pp. 348–374, Jan. 2021.
[33] Z. Sun, F. Li, X. Duan, L. Jin, Y. Lian, S. Liu, and K. Liu, "A novel adaptive iterative learning control approach and human-in-the-loop control pattern for lower limb rehabilitation robot in disturbances environment," *Auto. Robots*, vol. 45, no. 4, pp. 595–610, May 2021.
[34] L. Sun, X. Chen, and M. Tomizuka, "Selective iterative learning control with non-repetitive disturbance rejection," in *Proc. ISCIE/ASME Int. Symp. Flexible Automat.*, 2014, pp. 1–8.
[35] C. Lin, L. Sun, and M. Tomizuka, "Robust principal component analysis for iterative learning control of precision motion systems with non-repetitive disturbances," in *Proc. Amer. Control Conf. (ACC)*, Jul. 2015, pp. 2819–2824.
[36] C. Peng, L. Sun, and M. Tomizuka, "Constrained iterative learning control with PSO-Youla feedback tuning for building temperature control," *IFAC-PapersOnLine*, vol. 50, no. 1, pp. 3135–3141, 2017.
[37] B. H. Park, T.-Y. Kuc, and J. S. Lee, "Adaptive learning control of uncertain robotic systems," *Int. J. Control*, vol. 65, no. 5, pp. 725–744, Nov. 1996.
[38] A. Tayebi, "Adaptive iterative learning control for robot manipulators," *Automatica*, vol. 40, no. 7, pp. 1195–1203, Jul. 2004.
[39] C.-T. Hsu, C.-J. Chien, and C.-Y. Yao, "A new algorithm of adaptive iterative learning control for uncertain robotic systems," in *Proc. IEEE Int. Conf. Robot. Autom.*, Sep. 2003, pp. 4130–4135.
[40] S. Yang, X. Fan, and A. Luo, "Adaptive robust iterative learning control for uncertain robotic systems," in *Proc. 4th World Congr. Intell. Control Autom.*, Jun. 2002, pp. 964–968.
[41] R. Lee, L. Sun, Z. Wang, and M. Tomizuka, "Adaptive iterative learning control of robot manipulators for friction compensation," *IFAC-PapersOnLine*, vol. 52, no. 15, pp. 175–180, 2019.
[42] J.-X. Xu, B. Viswanathan, and Z. Qu, "Robust learning control for robotic manipulators with an extension to a class of non-linear systems," *Int. J. Control*, vol. 73, no. 10, pp. 858–870, Jan. 2000.
[43] J. Xu, "The fontiers of iterative learning control—Part II," *J. Syst. Control Inf.*, vol. 46, no. 5, pp. 233–243, 2002.
[44] A. Tayebi and C.-J. Chien, "A unified adaptive iterative learning control framework for uncertain nonlinear systems," *IEEE Trans. Autom. Control*, vol. 52, no. 10, pp. 1907–1913, Oct. 2007.
[45] X. He, H. Zhuang, D. Zhang, and Z. Qin, "Pulse neural network-based adaptive iterative learning control for uncertain robots," *Neural Comput. Appl.*, vol. 23, nos. 7–8, pp. 1885–1890, Dec. 2013.
[46] D. M. Dawson, C. Abdallah, and F. L. Lewis, *Robot Manipulator Control: Theory and Practice*. Upper Saddle River, NJ, USA: Prentice-Hall, 2004.
[47] H. K. Khalil, *Nonlinear Systems*, 3rd ed. Upper Saddle River, NJ, USA: Prentice-Hall, 2002.
[48] M. Wang, Y. Zhang, and C. Wang, "Learning from neural control for non-affine systems with full state constraints using command filtering," *Int. J. Control*, vol. 93, no. 10, pp. 2392–2406, Oct. 2020, doi: 10.1080/00207179.2018.1558285.
[49] J. Zhang, X. Liu, Y. Xia, Z. Zuo, and Y. Wang, "Disturbance observer-based integral sliding-mode control for systems with mismatched disturbances," *IEEE Trans. Ind. Electron.*, vol. 63, no. 11, pp. 7040–7048, Nov. 2016.
[50] J. Y. Lee, M. Jin, and P. H. Chang, "Variable PID gain tuning method using backstepping control with time-delay estimation and nonlinear damping," *IEEE Trans. Ind. Electron.*, vol. 61, no. 12, pp. 6975–6985, Dec. 2014.
[51] D. X. Ba, T. Q. Dinh, J. Bae, and K. K. Ahn, "An effective disturbance-observer-based nonlinear controller for a pump-controlled hydraulic system," *IEEE/ASME Trans. Mechatronics*, vol. 25, no. 1, pp. 32–43, Feb. 2020.
[52] Y. Wang, F. Yan, J. Chen, F. Ju, and B. Chen, "A new adaptive time-delay control scheme for cable-driven manipulators," *IEEE Trans. Ind. Informat.*, vol. 15, no. 6, pp. 3469–3481, Jun. 2019.
[53] A. K. Kostarigka and G. A. Rovithakis, "Prescribed performance output feedback/observer-free robust adaptive control of uncertain systems using neural networks," *IEEE Trans. Syst., Man, Cybern., B*, vol. 41, no. 6, pp. 1483–1494, Dec. 2011.
[54] S. Yin, H. Gao, J. Qiu, and O. Kaynak, "Descriptor reduced-order sliding mode observers design for switched systems with sensor and actuator faults," *Automatica*, vol. 76, pp. 282–292, Feb. 2017.
[55] H. Elci, R. W. Longman, M. Q. Phan, J.-N. Juang, and R. Ugoletti, "Simple learning control made practical by zero-phase filtering: Applications to robotics," *IEEE Trans. Circuits Syst. I, Fundam. Theory Appl.*, vol. 49, no. 6, pp. 753–767, Jun. 2002.
[56] R. Horowitz, "Learning control of robot manipulators," *J. Dyn. Syst. Meas. Control*, vol. 115, no. 2, pp. 402–411, 1993.
[57] B. E. Neubauer, C. T. Witkop, and L. Varpio, "How phenomenology can help us learn from the experiences of others," *Perspect. Med. Educ.*, vol. 8, no. 2, pp. 90–97, 2019.
[58] J. Mezirow, "A critical theory of adult learning and education," *Adult Educ.*, vol. 32, no. 1, pp. 3–24, 1981.
[59] J. Park and I.W. Sandberg, "Universal approximation using radial-basis-function networks," *Neural Comput.*, vol. 3, no. 2, pp. 246–257, Jun. 1991.
[60] F. L. Lewis, S. Jagannathan, and A. Jesildirek, *Neural Network Control of Robot Manipulators and Nonlinear Systems*. Boca Raton, FL, USA: CRC Press, 2020.
[61] D. X. Ba and T. T. Nguyen, "A new neural iterative learning control approach for position tracking control of robotic manipulators: Theory, simulation, and experiment," *Meas., Control, Autom.*, vol. 3, no. 2, pp. 66–74, 2022.
[62] H. Tao, J. Li, Y. Chen, V. Stojanovic, and H. Yang, "Robust point-to-point iterative learning control with trial-varying initial conditions," *IET Control Theory Appl.*, vol. 14, no. 19, pp. 3344–3350, Dec. 2020.
[63] G. Hinton, L. Deng, D. Yu, G. Dahl, A.-R. Mohamed, N. Jaitly, A. Senior, V. Vanhoucke, P. Nguyen, T. Sainath, and B. Kingsbury, "Deep neural networks for acoustic modeling in speech recognition: The shared views of four research groups," *IEEE Signal Process. Mag.*, vol. 29, no. 6, pp. 82–97, Nov. 2012.
[64] E. Akleman, "Deep learning," *Computer*, vol. 53, no. 9, p. 17, Sep. 2020.
[65] H. Nguyen and C. C. Cheah, "Analytic deep neural network-based robot control," *IEEE/ASME Trans. Mechatronics*, vol. 27, no. 4, pp. 2176–2184, Aug. 2022.
[66] X. Yang and X. Zheng, "Swing-up and stabilization control design for an underactuated rotary inverted pendulum system: Theory and experiments," *IEEE Trans. Ind. Electron.*, vol. 65, no. 9, pp. 7229–7238, Sep. 2018.
[67] N. Sunderhauf, O. Brock, W. Scheirer, R. Hadsell, D. Fox, J. Leitner, B. Upcroft, P. Abbeel, W. Burgard, M. Milford, and P. Corke, "The limits and potentials of deep learning for robotics," *Int. J. Robot. Res.*, vol. 37, nos. 4–5, pp. 405–420, Apr. 2018.

DANG XUAN BA (Member, IEEE) received the B.S. and M.S. degrees from the Ho Chi Minh City University of Technology, Ho Chi Minh City, Vietnam, in 2008 and 2012, respectively, and the Ph.D. degree from the School of Mechanical Engineering, University of Ulsan, Ulsan, South Korea, in 2016.

He is currently a Lecturer with the Department of Automatic Control, Ho Chi Minh City University of Technology and Education (HCMUTE), Vietnam, where he is also the Manager of the Dynamics and Robotic Control (DRC) Laboratory. His research interests include intelligent control, nonlinear control, modern control theories, and their applications in robotics.

NGUYEN TRUNG THIEN received the B.S. degree from the Hung Yen University of Technology, Hanoi, Vietnam, in 2005, the M.S. degree from the Hanoi City University of Technology, Hanoi, in 2010, and the Ph.D. degree from the School of Mechanical Engineering, University of Ulsan, Ulsan, South Korea, in 2016.

He is currently the Research and Development Director with Viettel Manufacturing Corporation, Vietnam. His research interests include mechanical aerospace systems and robotics.

JOONBUM BAE (Member, IEEE) received the B.S. degree in mechanical and aerospace engineering (summa cum laude) from Seoul National University, Seoul, South Korea, in 2006, and the M.S. degree in mechanical engineering, the M.A. degree in statistics, and the Ph.D. degree in mechanical engineering from the University of California at Berkeley, Berkeley, CA, USA, in 2008, 2010, and 2011, respectively. In 2012, he joined the Department of Mechanical Engineering, Ulsan National Institute of Science and Technology (UNIST), Ulsan, South Korea, where he is currently the Director of the Bio-Robotics and Control (BiRC) Laboratory. He was appointed as a Rising-Star Distinguished Professor of UNIST in 2018. He founded a startup Feel the Same, Inc., in 2017, which develops soft sensor systems. His current research interests include modeling, design, and control of human–robot interaction systems, soft robotics, and biologically inspired robot systems.

He was a recipient of the Samsung Scholarship for his Ph.D. studies. He received the Young Researcher Award from the Korea Robotics Society in 2015, the Korean Government Minister Award from the Ministry of Public Safety and Security and the Ministry of Science, ICT and Future Planning, in 2016 and 2017, respectively, and the Grand Prize from the UNIST Outstanding Faculty Awards in 2021. He led the Team UNIST at $10M ANA Avatar XPRIZE, which ranked sixth at the finals in 2022.